

**Lyudmila I. Nyrkova**

PhD candidat  
E.O.Paton Electric Welding Institute  
Department of gas and oil welding  
Kyiv,  
Ukraine

**Svetlana O. Osadchuk**

Junior researcher  
E.O.Paton Electric Welding Institute  
Department of gas and oil welding  
Kyiv,  
Ukraine

**Tetiana M. Labur**

Professor  
E.O.Paton Electric Welding Institute  
Department of physical and metallurgical  
processes of welding of light metals and  
alloys  
Kyiv,  
Ukraine

**Maria R. Yavorska**

Leading Engineer  
E.O.Paton Electric Welding Institute  
Department of physical and metallurgical  
processes of welding of light metals and  
alloys  
Kyiv,  
Ukraine

# Effect of Microstructure on Corrosion-Mechanical Endurance of Welded Joints of Aluminium Alloy V1341T Produced by Manual Argon-Arc Welding

*The results of microstructure effect on corrosion-mechanical endurance of 1.2 mm thick alloy of Al-Mg-Si-Cu alloying system and its welded joints, depending on their condition due to different types of HT are presented. Change of microstructure of the welded joints during performance of various HT operations practically does not affect its resistance against intergranular and exfoliating corrosion. Effect of HT on corrosion-mechanical endurance of welded joint under the conditions of simultaneous action of continuous loading and corrosive environment is ambiguous. Resistance against intergranular corrosion and corrosion cracking will determine the fracture resistance of welded products of V1341T alloy in service.*

**Keywords:** aluminum alloy of Al-Mg-Si-Cu system, welded joint, intergranular corrosion, exfoliating corrosion, corrosion cracking, corrosion-mechanical tests, potentiometry.

## 1. INTRODUCTION

Aluminium alloys of Al-Mg-Si-Cu alloying system, which are applied in aviation engineering, are characterized by high adaptability-to-fabrication in combination with the characteristics of strength, weldability and corrosion endurance [1, 2]. These alloys undergo cardinal microstructural changes during heat-strengthening treatment. The correlation between the heat treatment process, structure and properties of these alloys has been intensively studied recently [3, 4]. Optimization of ageing parameters is necessary to obtain a stable microstructure and to achieve the most favourable mechanical properties.

Mechanical and corrosion properties of the alloys are characterized by sensitivity of the structural components to temperature-time parameters of hardening and homogenizing operations, as this is exactly what affects the density of dispersoids in the metal [5]. Dispersoid crystals of  $\beta'$ -phase formed during delayed cooling act as anodes at contact with the corrosive environment. They dissolve and promote development of pitting as a result of disturbance of the passive film on the metal surface. In addition, precipitates of other phases, for instance  $[\beta(\text{Mg}_2\text{Si})$  and  $Q(\text{Al}_4\text{Si}_7\text{Mg}_8\text{Cu}_2)]$  can increase the structure sensitivity to the corrosive environment and development of intergranular corrosion (IGC) [6, 7].

It is known [2] that corrosion properties and residual life characteristics of the above alloys affect the geometrical dimensions of microstructure grains, phase arrange-

ment and local stressed state of the metal. As evidenced by the data of works [8-10], application of aluminium alloy heat treatment increases the level of their mechanical properties. So, alloy heat treatment to T6 (ageing) and T73 (hardening and artificial ageing) conditions improves the strength properties due to a change of the shape of secondary strengthening phases and their more uniform distribution in the metal volume, that also promotes increase of corrosion resistance. Moreover, low-temperature modes of thermomechanical treatment or multistage artificial ageing to T78 condition are used under production conditions, in order to increase the alloy resistance to intergranular corrosion [11]. Thus, application of different processes of heat treatment of alloys of Al-Mg-Si-Cu system allows increasing their strength level. Strength models were developed for optimization of ageing parameters [12, 13].

In work [14] a correlation is established between temperature, heat treatment duration, and hardness of alloys of Al-Mg-Si system, which can be used for selection of ageing parameters, in order to achieve the set level of mechanical strength.

Results of studying the effect of ageing temperature on mechanical properties of Al-Mg-Si alloy [15] showed that at low-temperature ageing (160 °C) ductility and impact toughness are high, whereas at 180 °C much higher values of ultimate tensile strength and hardness were obtained, compared to values obtained at 160 °C. It is also noted that the ageing temperature affects formation of  $\text{Mg}_2\text{Si}$  intermetallic inclusions of Al-Mg-Si alloy and its microstructure: ageing at 180 °C for 8 hours favours uniform distribution of  $\text{Mg}_2\text{Si}$  intermetallic phases by solid solution strengthening that allows achieving higher mechanical properties than those obtained at 160 °C. Relative elongation and impact energy decrease with increase of ageing temperature, whereas the strength and ductility limit and hardness increase, on the contrary.

Received: December 2020, Accepted: February 2021

Correspondence to: Dr Lyudmila Nyrkova  
E.O. Paton Electric Welding Institute,  
Department of gas and oil welding, Kazymir Malevich  
Str., 11, 11120 Kyiv-150, Ukraine  
E-mail: lnyrkova@gmail.com.ua, nyrkova@paton.kiev.ua

doi:10.5937/fme2102374N

© Faculty of Mechanical Engineering, Belgrade. All rights reserved

Studying the effect of heat-treatment at 175 °C for different times on the microstructure and mechanical properties showed that the optimum ageing duration is soaking for 3 to 5 hours, during which the fine-grained structure forms and the highest mechanical properties are achieved [16]. With increase of ageing time, the quantity and size of the phases are increased and the mechanical characteristics decrease, accordingly.

In work [17], the results of studying artificial ageing in the temperature range of (155–350) °C for (2-100) hours are given, and it is proposed to assess the effect of ageing modes on strength and yield values, using diagrams of empirical quality characteristic  $Q$ . It is shown that  $Q$  is more sensitive to the change of ductility limit than to the change of the strength limit. The shape of diagrams of quality index  $Q$  is related to a change of the strength and yield limit, as a result of the impact of ageing time and temperature on dispersion strengthening of the copper phase.

The group of aluminium alloys of Al-Mg-Si-Cu alloying system includes the alloy of V1341 grade, which is used for manufacturing cylinders, and tanks for storing liquids in aviation equipment [18]. The need to ensure the optimum level of both mechanical and corrosion properties is associated exactly with it. The parts of hydraulic tanks are often joined by manual argon-arc welding after stamping. Weld metal resistance usually does not match that of the base metal, primarily because of the inhomogeneity of the welding consumable composition.

As one can see from the given review, the data of experimental studies mostly concern the base metal, but HT effect on the corrosion-mechanical properties of welded joints of these alloys is insufficiently studied. Therefore, the objective of this work is investigation of the effect of the structure on a set of corrosion and corrosion-mechanical properties of welded joints of V1341T alloy, in order to search for an effective technological process of fabrication of such structures by the technology of manual argon-arc welding.

Thus, the data presented in the literature focus on the study of individual properties of the alloy B1341 (mechanical, structural or corrosive), the information on the complex of its properties is very limited. Moreover, data on the complex properties of the welded joint were not found.

Whereas the welding mode must be selected separately for each thickness of the sheet which will be welded, the resulting welded joint is a new material with its own properties. The uniqueness of this work is that the optimal mode of welding of thin-sheet semi-finished product with a thickness of 1.2 mm is found, the acceptable mode of heat treatment is determined. This made it possible to obtain a welded joint with high mechanical properties, to comprehensively assess the corrosion and mechanical strength of the joint, based on which to identify the most important factors that will determine the resistance to destruction of welded products of this alloy during operation. This is the practical significance of the work.

## 2. EXPERIMENTAL PROCEDURE

Aluminium alloy of Al-Mg-Si-Cu alloying system of V1341T grade was used in the work. The alloy chemical

composition which was determined by the method of spectral analysis in DFS-36 spectrometer, was as follows, (wt.) %: (0.45-0.9) Mg, (0.5-1.2) Si, (0.15-0.35) Mn, (0.1-0.5) Cu, (0.05-0.1) Ca, (0.25 Cr, 0.2 Zn, 0.15 Ti, 0.5 Fe, other elements being not more than 0.1.

Sheet blanks of V1341T alloy 1.2 mm thick were etched before welding in 10 % solution of NaOH and clarified in 25 % solution of HNO<sub>3</sub>, thoroughly rinsed in running hot and cold tap water, and dried in air. Billet edges were mechanically scraped to the depth of 0.1 mm. Welding of butt welds was performed along the rolling direction of sheet semi-finished products.

Sheet blanks were butt welded, without backing, by single-pass manual welding with filler wire Sv 1217 of 1.2 mm diameter in argon shielding gas (in keeping with GOST 10157 [19]). Welding was performed by a free-burning arc with different-polarity current of a sinusoidal shape, using MW2000 inverter of Fronius Company. Searching for an optimum welding technology is described in work [20]. The following mode was recognized as optimum for welding the studied alloy:  $I_w=54-56$  A,  $U_a=11.1-12.4$  V, in which a tight weld without defects is formed. Appearance of the welded joint is given in Figure 1.

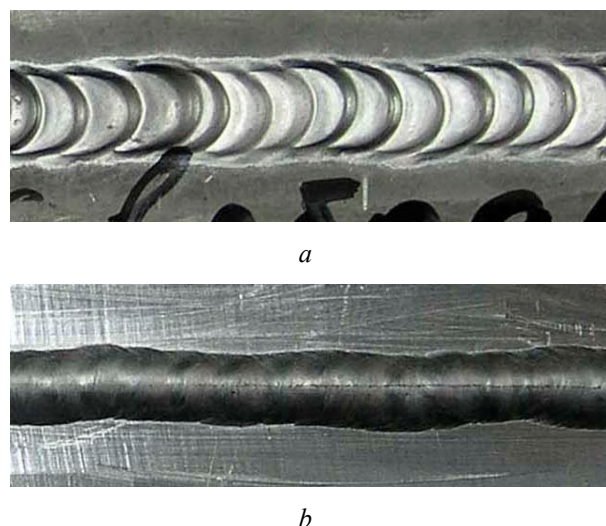


**Figure 1. Appearance of welded joint in as-welded condition: 1 – weld face; 2 – weld root**

After welding, the hot cracking susceptibility of the welded joint was evaluated using Houldcroft samples [21]. Quality of butt joints was controlled visually and by roentgenography method [22] in RAP-150/300 unit. The density of weld metal structure was determined in «Densitometer» instrument.

Figure 2 shows the scheme of performance of operations of the studied sample heat treatment and their modes.

Determination and evaluation of mechanical properties were performed on flat samples with technological reinforcement on the face and reverse sides of the weld. Mechanical testing was conducted in [23, 24] in Instron-1126 machine. Extensometer № G-51-12-M-A was used to control the value of relative elongation of the samples. Loading was performed with 6 mm/min speed of the traverse movement up to fracture. During testing the load and deformation values were recorded continu-

ously, and the results were used to calculate the respective values of yield limit, tensile strength (strength limit) and relative elongation. Deformability of the base metal and welded joints was evaluated by bend angle value ( $\alpha$ ) at three-point bending with load application from the weld root side, in keeping with GOST 6996 [24].

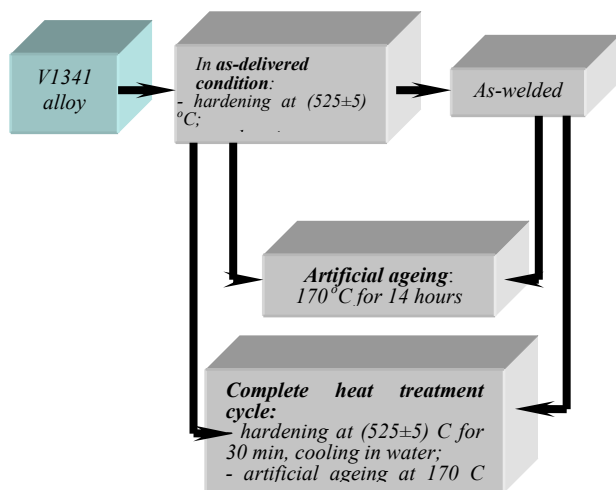


**Figure 2. Scheme of the sequence of operations of the studied samples heat treatment and their modes.**

Welded joint microstructure was studied on metallographic sections cut out normal to the weld axis. Sections were prepared by a standard procedure. In order to reveal the microstructure, electrolytic etching in a solution of the following composition: 930 ml  $\text{CH}_3\text{COOH}$  + 70 ml  $\text{HClO}_4$ , was used.

Electrochemical studies were conducted by the methods of potentiometry and polarization curves, using PI-50-1.1 potentiostat and Pr-8 programmer. Potential distribution over the welded joint surface was studied by the method of measurement of the potential under the drop in 3 % NaCl solution by the E.O.Paton Electric Welding Institute procedure. Clamp electrochemical cell was used for investigation of the polarization curves. The working electrode were different zones of the welded joint, reference electrode was a saturated silver chloride electrode EVL-1M1, and additional electrode was platinum. Polarization curves were recorded in a potentiodynamic mode, with the potential scanning speed of 0.5 mV/s in 3 % NaCl solution. Before measurement, the sample surface was treated with sanding paper and degreased with ethyl alcohol.

Resistance to intergranular corrosion (IGC) and exfoliating corrosion was tested by standard procedures to GOST 9.021 [25] and GOST 9.904 [26].

Corrosion cracking resistance was studied in keeping with GOST 9.019[27]. Sample testing was conducted under continuous axial tensile loading on the level of 160 MPa at complete immersion into 3 % NaCl solution in «Signal» unit. The weld was located normal to the loading vector. Testing duration was not less than 45 days.

### 3. RESULTS AND DISCUSSION

#### 3.1 Microstructural studies

**Condition in as-delivered condition (hardening and natural ageing).** In the heat-affected zone (HAZ) struc-

tural and phase transformations occur under the impact of the thermal cycle of welding, namely: increase of grain size, complete or partial lowering of the effect of metal hardening after natural ageing, local annealing and hardening of individual regions. Interaction of boundary intermetallic inclusions with the solid solution here leads to formation of regions with liquid interlayers of low-melting eutectics along the grain boundaries, Figure 3, a.

**Condition after artificial ageing.** Formation of wider grain boundaries due to precipitation of additional phases, which strengthen the metal, and coarsening of intermetallic phases through their combination, are found in the weld structure, Figure 3, b.

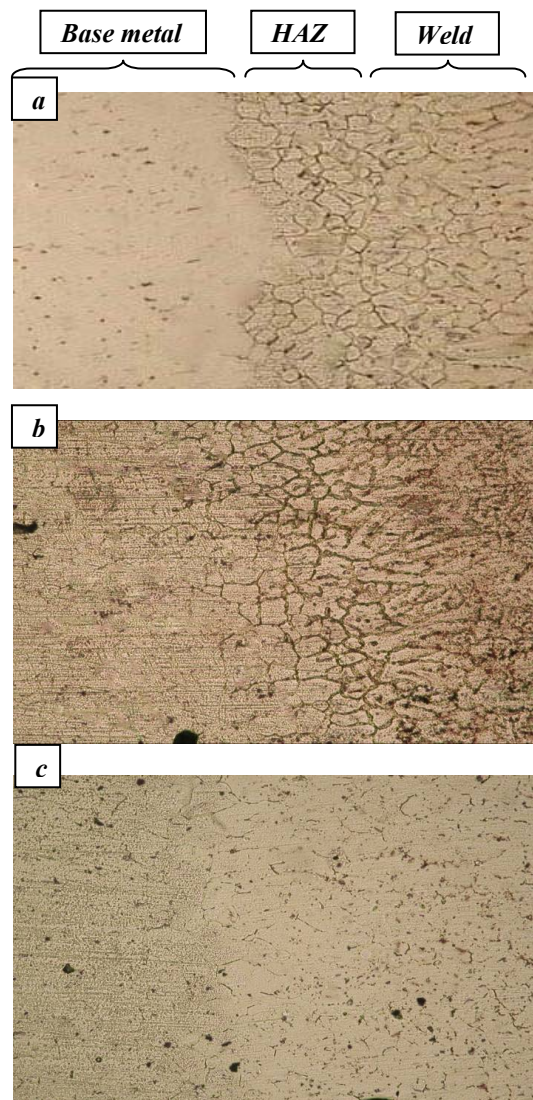


**Figure 3. Microstructure of a welded joint of V1341T alloy in different conditions: a – in as-delivered condition (hardening and natural ageing); b – after artificial ageing; c – after hardening and artificial ageing,  $\times 320$ .**

Structural change is the result of solid solution decomposition, dispersion hardening of phases, and increase of volume fraction of these phases, because of increase of their density, Figure 3, b. The process is accompanied by thickening of the grain boundaries, as a result of their possible contact fusion with each other and with  $\text{Mg}_2\text{Si}$  eutectic phase, which is located near the grain boundaries. A change of geometrical dimensions

of the structural components occurs in the HAZ metal: increase of grain size and coagulation of insoluble phase inclusions.

**Condition after hardening and artificial ageing.**

Conducting a complete HT cycle leads to a change of parameters of the structural components (geometrical dimensions of the grains, width of interlayers between them, precipitation of additional phase inclusions, etc.) in the regions that were exposed to technological heating during welding, Figure 3, c. We note formation of thinner boundaries of the structural components, alongside equalizing of the nature of phase precipitate distribution along the grain boundaries, due to a fast fixing of dispersed dimensions of phase precipitates (Figure 3, c). They are associated with presence of small additives of copper (0.3%) in the alloy that, in keeping with the data of [2], limits the rate of precipitation of Guinier-Preston zones, which are in metastable equilibrium with the solid solution. Distribution of phase precipitates in the matrix is of a more uniform nature, however, phase dimensions are more dispersed. This is influenced by fast fixation of the structural components during water quenching. At the stage of artificial ageing, which follows hardening, the shape and dispersed dimensions of the structural components are preserved. Moreover, thickening of the boundaries of crystallites and grains is observed in some regions, in particular in the zone of the weld fusion with the base metal. Their total thickness, however, is smaller than in the structure of welded joints after artificial ageing (Figure 3, b).

**3.2 Mechanical studies**

Mechanical properties of the samples with different microstructure, depending on their condition, are given in Figure 4.

**As-delivered condition (hardening and natural ageing).** Metallographic investigations showed that the microstructure of base metal of V1341T alloy consists of saturated solid solution, Mg<sub>2</sub>Si phase precipitates and coarse inclusions of insoluble intermetallics, which penetrate into the metal at the metallurgical stage of semi-finished product fabrication (Figure 3, a).

As one can see from Figure 3, during arc welding of V1341T alloy structural transformations take place in the metal, leading to formation of three structural zones: weld (Figure 3, c), fusion zone and heat-affected zone (Figure 3, b). The structure of welds in the samples in as-welded condition is uniform with characteristic phase arrangement, and it consists of fine dendrites (Figure 3, c). There are no coarse defects or discontinuities in the weld volume.

Coagulation of inclusions along the grain boundaries increases the inter-phase distance. Columnar crystallites are found near the line of weld fusion with the base metal, as a result of rapid heat removal and metal solidification. These crystals are oriented parallel to the direction of metal melting vector during welding, Figure 3, b. From the base metal side, decomposition of oversaturated solid solution, simultaneous precipitation and dissolution of earlier formed strengthening phases take place in the fusion zone. This is accompanied by coagulation

(enlargement) of insoluble intermetallic phases, which form at the stage of metallurgical production and can promote increase of stresses in the structure. [3].

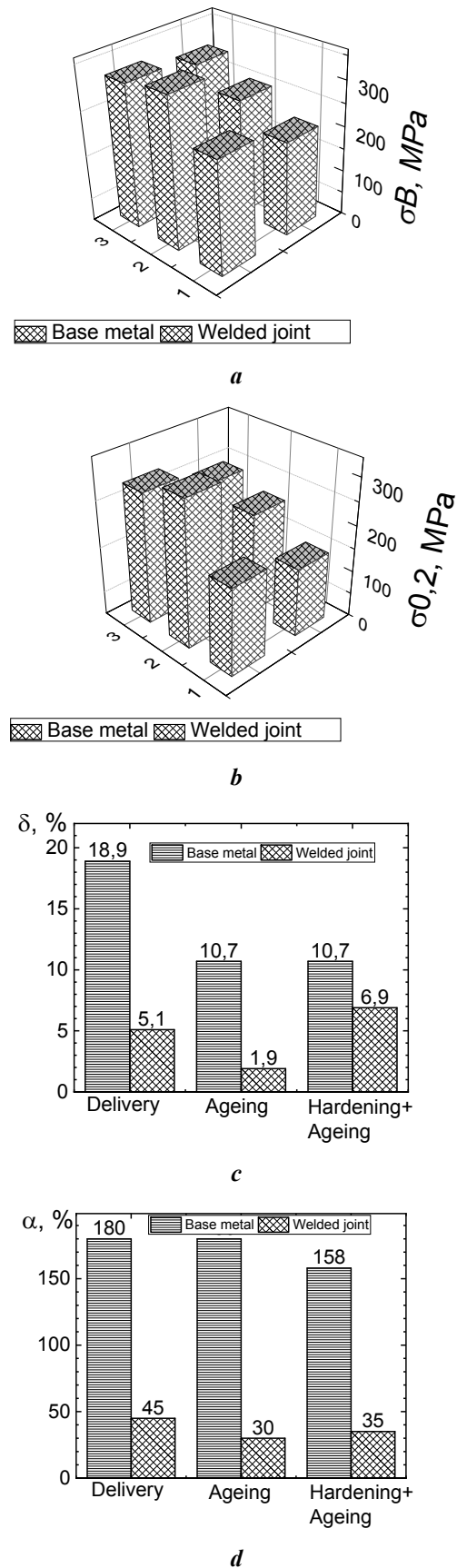


**Figure 4. Mechanical properties of base metal and welded joints in as-delivered condition (1), after artificial ageing (2) and after complete heat treatment cycle (3): a – strength limit; b – yield limit; c – relative elongation; d – bend angle.**

Analysis of test results showed that base metal samples (after welding, after artificial ageing, after hardening and artificial ageing) fail in the work zone, and failure of welded joint samples after similar HT operations occurs in the HAZ at 3-5 mm distance from the fusion boundary. This is associated with metal softening under the impact of the thermal cycle of welding. Level of mechanical properties of V1341T alloy depends directly on the arrangement of structural components as a result of the respective transformations in the metal during welding or HT (Figure 4).

Compared to strength values of the base metal in a similar heat-treated condition, the level of these characteristics of the welded joints is lower, Figure 4: welded joint strength limit changes from 208.7 (as-delivered condition) to 257.6 (after artificial ageing) and 299.6 MPa (after hardening and artificial ageing), yield limit changes from 147.5 to 215.5 and 241.5 MPa, respectively. Strength factor of welded joints in the above-mentioned conditions is equal to 0.83, 0.77 and 0.93, respectively. Relative elongation of welded joints is equal to: 5.1 % (as-delivered condition), minimum value of relative elongation was determined to be 1.9 % for samples after artificial ageing, after complete HT cycle an increase of this value to 6.9 % was observed, Table 1. Base metal bend angle in as-delivered condition and after artificial ageing is 180 °, after complete HT cycle it is 138°. For welded joints, this value is considerably smaller and equal to 45, 30 and 32°, respectively.

**Table 1. Mechanical properties of the base metal and welded joints of V1341T alloy in different conditions**

Condition of the sample	Properties of base metal and welded joints				
	Mechanical				
	$\sigma_b$ , MPa	$\sigma_{0.2}$ , MPa	$\delta$ , %	$\alpha$ , degr.	Strength factor of WJ
<i>Base metal</i>					
As-delivered condition (hardening + natural ageing)	250.5	187.6	18.9	180	-
Artificial ageing	335.7	313.3	10.7	180	-
Hardening + artificial ageing	321.1	282.0	10.7	158	-
<i>Welded joint</i>					
As-delivered condition (hardening+ artificial ageing)	208.7	147.5	5.1	45	0.83
Artificial ageing	257.6	215.5	1.9	30	0.77
Hardening + artificial aging	299.6	241.5	6.9	35	0.93

Fracture of welded joint samples occurs both along the fusion boundary of the weld and base metal, and in the HAZ region at 5 mm distance from the boundary. The first can be caused by metal overheating during performance of manual welding, and the second – by a considerable quantity of phases, precipitating under the artificial ageing conditions, as well as a result of coagulation of coarse particles of intermetallic phases,

which together form a continuous network around the grains. Its presence leads to an abrupt lowering of ductility values. The noted fact should be taken into account during selection of the mode of heat treatment of V1341T alloy welded joints under industrial conditions of welded structure fabrication.

After artificial ageing of the welded joint, an increase of the values of strength and yield limit to 277 and 232 MPa is observed (Table 1). The strength factor of the joints is equal to 0.84 on average. However, the relative elongation value is 1.9 % that is almost 10 smaller than that of the base metal in a similar condition. The value of bend angle of the welded joints is equal to 30 degr.

After performance of the complete HT cycle (hardening + artificial ageing) the strength value of welded joints is equal to 300 MPa, and that of yield limit is 265.5 MPa (Table 1). Their strength coefficient is equal to 0.93 of base metal level. Relative elongation value, even though it is two times smaller than similar values of the base metal, is on the level of 10.7%. Bend angle is equal to 158 °. This is due to reduction of the dimensions of phase precipitates under the conditions of performance of the complete HT cycle at preservation of their quantity that promotes an extensive nature of plastic deformation of metal. Fracture mode of the samples, similar to the previous case, is also nonuniform along the fusion boundary and in base metal regions in the HAZ, where annealing occurred during technological heating of the welded joint. The established fact can also be related both to base metal quality, and to stability of manual arc welding process performance.

Thus, heat treatment of welded joints of V1341T alloy, which includes hardening and artificial ageing, allows producing a more uniform structure. It can be assumed that such a structure of the joint will be resistant to corrosion damage at a high strength level, compared to the mode of just artificial ageing. This is due to the dimensions of phase precipitates and their density in the metal that affects the stress level in the structure. Presence of finer phases, uniformly arranged in the bulk of the weld crystallites and base metal grains, promotes uniform deformation and does not cause any stress localization on their boundaries. This is exactly what determines the high level of stress corrosion resistance. In other words, the complete heat treatment cycle is an effective means to improve the structure and corrosion-mechanical properties of the welded joints.

### 3.3 Electrochemical investigations

Corrosion potential of the base metal in as-delivered condition is equal to -0.729 V. Potential difference between the base metal and HAZ is equal to 0.028 V, between the base metal and weld it is 0.099 V, Figure 5 (curve 1).

After artificial ageing, shifting of base metal corrosion potential to more positive values, to -0.718 V, is observed, compared to as-delivered condition. For this welded joint, the difference of potentials is equal to: 0.010 V between base metal and HAZ, 0.048 V between base metal and weld, Figure 5 (curve 2). After a complete HT cycle, the base metal corrosion potential again becomes almost the same, as in as-delivered condition,

being -0.73 V. The difference of potentials between base metal and HAZ is equal to 0.020 V, between base metal and weld it is 0.043 V, Figure 5 (curve 3).

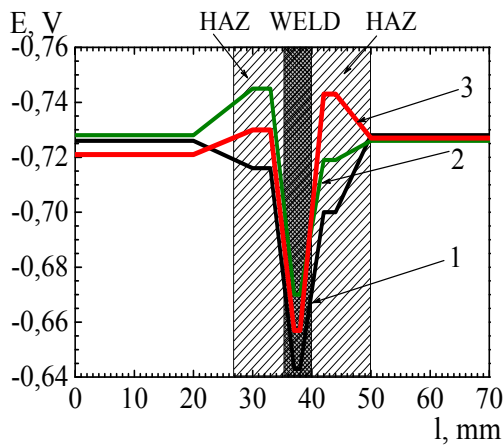


**Figure 5.** Nature of potential distribution under the drop in different zones of welded joints of V1341T alloy in different conditions: 1 – as-delivered; 2 – after artificial ageing; 3 – after quenching and artificial ageing.

Analysis of the obtained results shows that for a welded joint in as-delivered condition there exists an electrochemical heterogeneity, as the difference of potentials between the base metal and weld is higher than the value admissible by GOST 9.005 for the welded joints and is equal to (0.71-0.67) V. It should be noted that in this joint the HAZ also has a more negative potential, compared to the weld, and, as its area is commensurate with that of the weld, such a potential distribution presents the risk of a more active dissolution of this zone. That is, after heat treatment a reduction of the potential difference between the weld and the HAZ is observed: after artificial ageing – to values of (0.021-0.063) V, after complete heat treatment cycle – to (0.038-0.064) V. However, the difference of potentials remains higher than the admissible one that should be taken into account during product service.

Polarization curves, measured on the base metal and weld, are given in Figure 6.

Curve analysis shows that the anode dissolution current on a weld of samples in as-delivered condition and after artificial ageing (Figure 6, a, b) is much higher than on the base metal. It correlates with the above statement that the metal sensitivity to the environment is also affected by appearance of coarse inclusions of intermetallic phases during the thermal cycle of welding,

Figure 6, that causes an increase of stress concentration in the metal. Therefore, the susceptibility to predominantly anode dissolution at contact with the environment is determined by electrochemical heterogeneity of the structure of different welded joint zones, in which intermetallic phases, formed by alloying elements, precipitate.

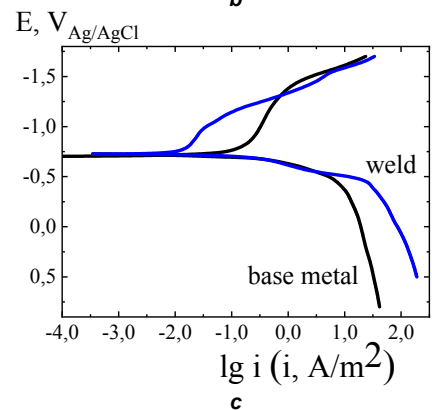
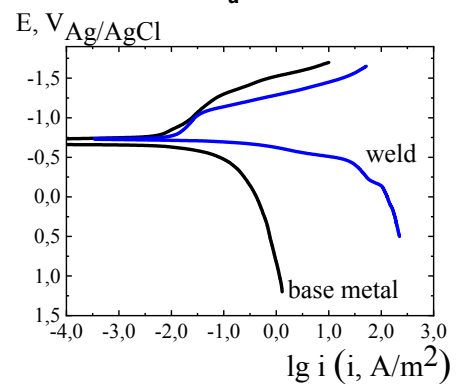
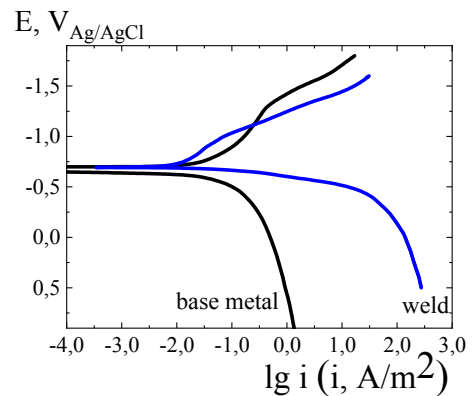
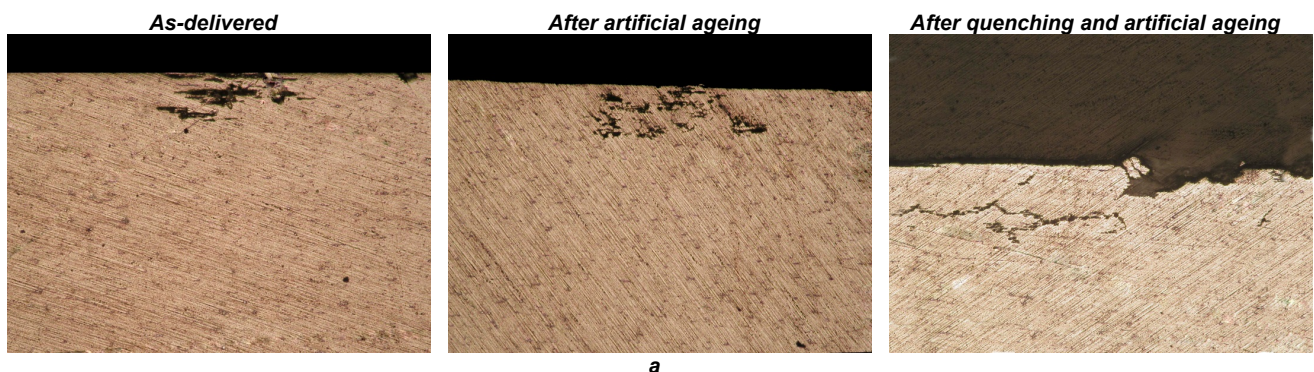


**Figure 6.** Polarization curves of the base metal and weld obtained on V1341T alloy in different conditions: a – as-delivered; b – after artificial ageing; c – after quenching and artificial ageing.



a

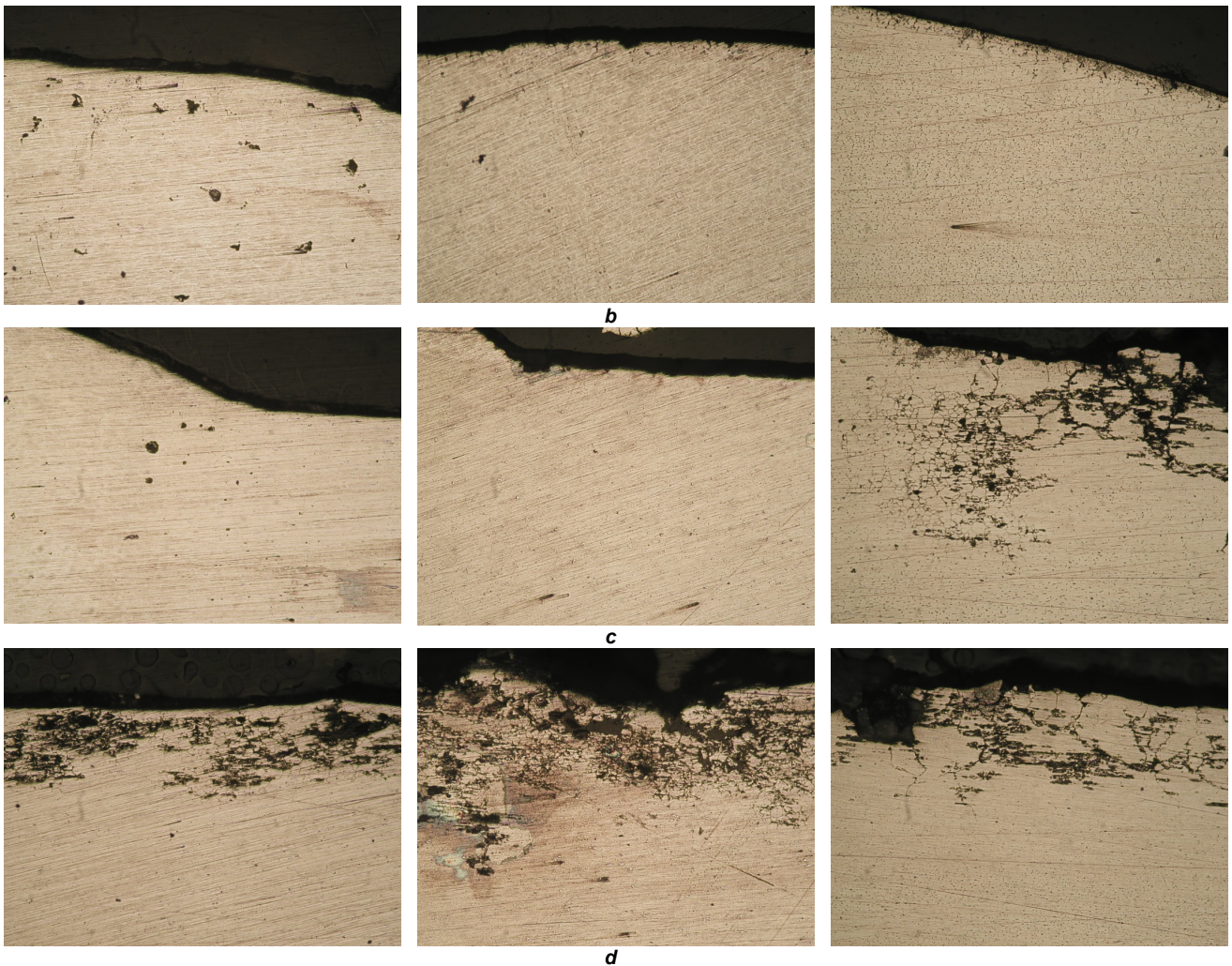


Figure 7. Microstructure of zones of V1341T alloy welded joint after testing for intergranular corrosion endurance,  $\times 320$ : a – base metal; b – weld; c – fusion zone; d – HAZ.

### 3.4 Intergranular corrosion resistance

Investigations of intergranular corrosion (IGC) resistance of the base metal in as-delivered condition showed that the depth of damage of the grain boundaries varies from 0.082 to 0.086 mm (Table 2).

Intergranular fracture in the welded joint in as-welded condition was not observed in the area of the weld and the fusion zone (Fig. 7, b, c), but the depth of grain boundary damage in the HAZ (Figure 7, d) was equal from 0.245 to 0.350 mm. Increase of IGC susceptibility of the welded joint is attributable to appearance of coarse inclusions of intermetallic phases during the thermal cycle of welding that caused an increase of stress concentration in the metal. Formation of regions of electrochemical heterogeneity in the welded joint structure, in which intermetallic phases from alloying elements precipitated, led to development of intergranular fracture. Therefore, the mechanism of intergranular fracture is related to the process of precipitation of secondary phases, formed by alloying elements, and depletion of solid solution composition. Obtained data correlate with the results of work [7].

After HT an increase of the depth of intergranular fracture of the base metal was observed (Figure 7, a): after artificial ageing – to (0.074-0.111) mm, after complete HT cycle – to (0.111-0.209) mm (Figure 8, a).

Table 2. Corrosion and corrosion-mechanical properties of the base metal and welded joints of V1341T alloy in different conditions

Condition of the sample	Depth of intergranular corrosion, mm	Resistance to exfoliating corrosion, point	Fracture time, days
<i>Base metal</i>			
As-delivered condition (hardening + natural ageing)	from 0.082 to 0.086	2-3	from 67 to 88
Artificial ageing	from 0.074 to 0.117	2-3	from 47 to 77
Hardening + artificial ageing	from 0.111 to 0.209	2-3	from 45 to 87
<i>Welded joint</i>			
As-delivered condition (hardening + artificial ageing)	from 0.245 to 0.350	1	from 1 to 49
Artificial ageing	from 0.123 to 0.301	1	from 3 to 9
Hardening + artificial ageing	from 0.214 to 0.287	1	from 4 to 54

No intergranular fracture was observed in the weld (Figure 7, b) of welded joints in all the conditions. Intergranular fracture is also absent in the fusion zone of the

welded joints in as-delivered condition and after artificial ageing, Figure 7, c. After the complete heat treatment cycle, however, intergranular fracture developed in the welded joint from the fusion zone to the HAZ (Figure 7, c) to the depth of 0.214 to 0.287 mm, Figure 8.

Intergranular corrosion of the welded joint in the condition after artificial ageing propagated through the HAZ (Figure 7, d), its depth being from 0.142 to 0.300 mm, Figure 8, a.

Thus, performance of HT by different modes reduces the IGC resistance of the base metal, but the depth of damage of the grain boundaries does not exceed the admissible value (0.350 mm). HT practically does not change the IGC resistance of welded joints of V1341 alloy.

### 3.5 Resistance to exfoliating corrosion

Resistance of samples of V1341T alloy welded joints to exfoliating corrosion does not deteriorate after heat treatment, Figure 9.

In the base metal (in as-delivered condition, after artificial ageing, after hardening and artificial ageing) delaminations of not more than 1 mm diameter are noted. Area of delaminations on base metal surfaces (in as-delivered condition, and after hardening and artificial ageing) does not exceed 1.5%, after artificial ageing – 1.0 %. No delaminations were revealed on the end faces in any of the samples. Delaminations were also absent in the HAZ and on the weld.

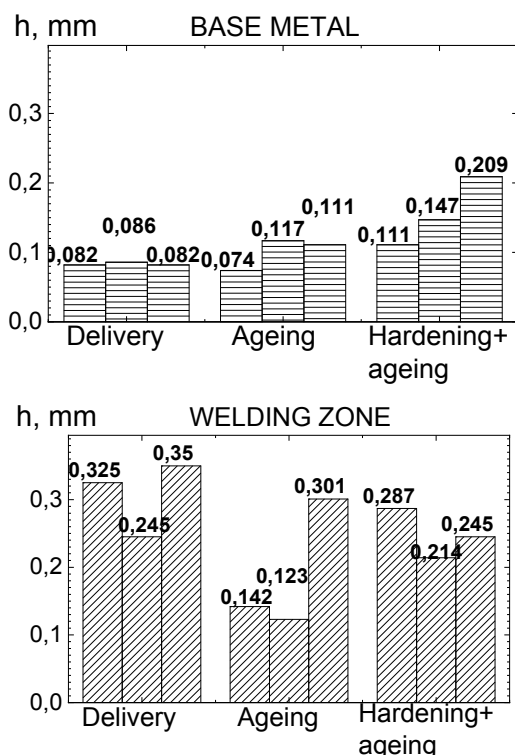


**Figure 8. Depth of intergranular corrosion of base metal and fusion zone of welded joint of V1341T alloy in different conditions**

According to GOST 9.904, the exfoliating corrosion resistance of samples of welded joint of V1341T alloy (in as-delivered condition, after artificial ageing, after quenching and artificial ageing) was estimated by 2-3 points by a ten point scale, Table 2.

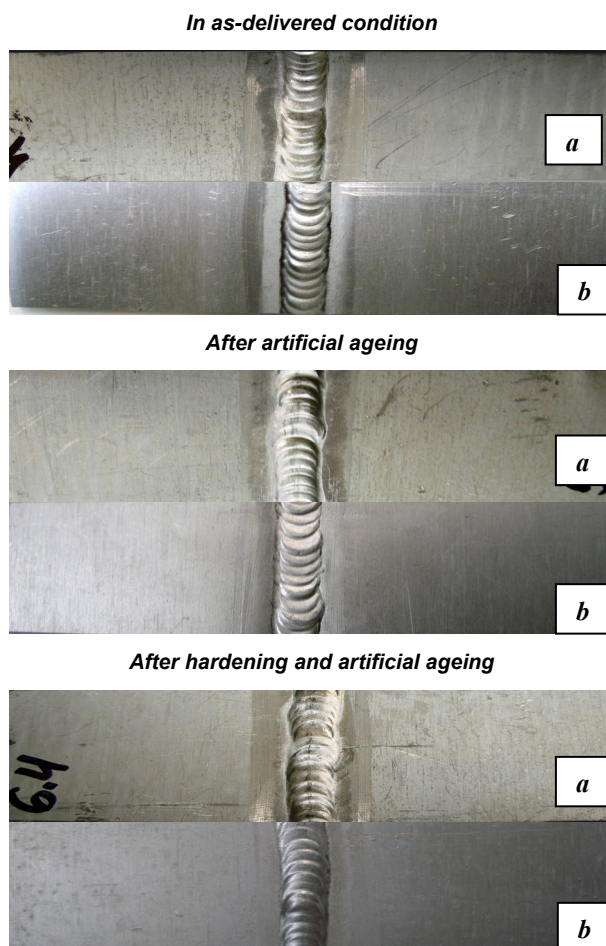


**Figure 9. Photo of welded joint samples before (a) and after (b) testing for resistance to exfoliating corrosion.**

### 3.6 Resistance to corrosion cracking corrosion

HT impact on corrosion-mechanical endurance of base metal and welded joints under the conditions of simultaneous action of continuous loading at complete immersion into the corrosive environment is ambiguous. Appearance of samples after testing is shown in Figure 10, a, b. A rather considerable scatter of experimental data is observed.

Time-to-fracture of welded joint samples in as-welded condition was from 10 to 46 days (20 days on average) that is almost three times less than that of the base metal - from 67 to 88 days (approximately 73 days) (Table 2). It is obvious that acceleration of welded joint failure, compared to the base metal, is due to increase of the grain size and local annealing and hardening of individual regions.

After HT a slight reduction of time-to-fracture occurs in base metal samples: after artificial ageing – to (47-77) days, after complete cycle – to (45-77) days. That is, after heat treatment (both after artificial ageing, and after hardening with subsequent artificial ageing) the corrosion-mechanical resistance of the base metal decreases by approximately (12-33) %.

For the welded joint an essential lowering of resistance to corrosion-mechanical fracture after artificial ageing – to (3-9) days, was observed. After a complete heat treatment cycle, however, the time-to-fracture somewhat increased to 54 hours, compared to as-welded



condition. Increase of resistance to corrosion-mechanical failure correlates quite well with the uniformity of microstructure, which was produced at complete HT cycle.

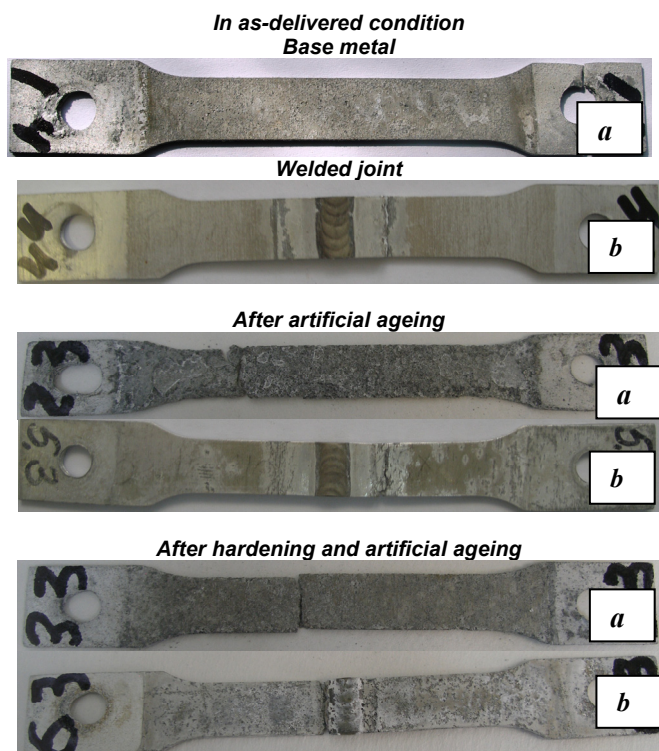


**Figure 10.** Photo of samples of base metal and welded joint after testing for resistance to corrosion cracking.

Pits formed on the sample surface, their quantity being greater for the heat-treated samples that pointed to certain differences in the structure heterogeneity. On welded joint samples pitting is concentrated predominantly in the HAZ that may be indicative of corrosion localizing exactly in this part of the alloy welded joints.

#### 4. CONCLUSIONS

Results of studying the structure of V1341 alloy 1.2 mm thick show the metal sensitivity to HT types that determines the level of its mechanical and corrosion properties.

1. It is established that sound welds are produced during nonconsumable-electrode manual welding of V1341T alloy using filler wire of Zv1217 grade. Heat treatment increases the level of strength of welded joints by 50 and 90 MPa and of yield point by 70 and 90 MPa, but HT impact on relative elongation is ambiguous: relative elongation decreases by approximately 3 times after artificial ageing and increases by approximately 35 % after the complete HT cycle. Bend angle after both HT modes decreases by 15 to 10 degrees, compared with as-welded condition. This is related to a considerable quantity of phases, which precipitate along the grain boundaries under the conditions of artificial ageing, as well as enlargement (coagulation) of coarse particles of insoluble intermetallic phases.

2. Heat treatment effect on corrosion-mechanical endurance of the base metal and welded joint under the conditions of simultaneous impact of continuous load and corrosive environment (at complete immersion) is

ambiguous. After HT reduction of the base metal time-to-fracture by approximately (12-33) % occurs: from (67-88) days in as-delivered condition to (47-77) days after artificial ageing and to (45-77) days after the complete HT cycle. Resistance to corrosion-mechanical failure of the welded joint decreases significantly after artificial ageing (to (3-9) days), but after the complete heat treatment cycle time-to-fracture increases to 54 hours, compared with the as-welded condition, which was (10-49) days.

3. Corrosion-mechanical resistance of the welded product after the complete HT cycle depends on the dimensions of the structural components and their arrangement in different zones of the welded joints. Therefore, these are exactly the values of intergranular fracture and corrosion cracking on the whole which can characterize the cracking sensitivity of welded joints of V1341 alloy. These factors will probably have the strongest effect on the products in service.

#### ACKNOWLEDGEMENTS

The work was carried out within the framework of the departmental order program of the National Academy of Sciences of Ukraine by the E.O. Paton Electric Welding Institute in 2017-2019 (fundamental research works) «Establishment of regularities of corrosion resistance increase of welded joints of structural aluminum alloys of different alloying systems produced by fusion and solid-phase welding technologies for aviation and marine transport» (State registration number 0117U001188).

#### REFERENCES

- [1] Feigenbaum Yu.M., Dubinskii S.V. Effect of accidental service damage on the strength and residual life of aircraft structures, *Scientific Bulletin of Moscow State Technical University of Civil Aviation*. Vol. 187, 83–91, 2013.
- [2] Klochkov G.G., Klochkova Yu.Yu., Romanenko V.A. Effect of deformation temperature on the structure and properties of extrusions from V-1341 alloy of Al-Mg-Si system. *Proc. of VIAM*. Vol. 9, pp. 3–11, 2013.
- [3] Murayama M., Hono K., Saga M., Kikuchi M. Atom probe studies on the early stages of precipitation in Al–Mg–Si alloys. *Mater. Sci. Eng. A*. Vol. 250, pp. 127-132, 1998.
- [4] Pogatscher S., Antrekowitsch H., Leitner H., Sologubenko A.S., Uggowitzer P.J. Influence of the thermal route on the peak-aged microstructures in an Al–Mg–Si aluminum alloy. *Scripta Mater.* Vo. 68, pp. 158-161, 2013.
- [5] Wang S., Matsuda K., Kawabata T., Ikeno S. Variation of Ageing Behavior for Al–Mg–Si. Alloys with Different TMs Addition, in: *Proceedings of the 12th International Conference on Aluminium Alloys, 05-09.09.2010*, Yokohama, pp. 2008–2011.
- [6] Kablov E.N. Aviation materials science in the XXI century. Prospects and objectives. Aviation materials, in: *Selected works. Jubilee Scientific-Technical Collection: (Ed.): M.: MISIS, VIAM*, p. 25, 2002.

- [7] Labisz K., Krupiński M., Dobrzański L.A. Phases morphology and distribution of the Al-Si-Cu alloy. *Journal of Achievements of Materials and Manufacturing Engineering*, Vol. 2, pp. 309-316, 2009.
- [8] Vijaya Kumar P., Madhusudhan G., Reddy K., Srinivasa Rao. Microstructure, mechanical and corrosion behavior of high strength AA7075 aluminium alloy friction stir welds - Effect of post weld heat treatment. *J. Defence Technology*. Vol. 11, 362-369, 2015.
- [9] Gharavi F., Matoria K.A., Yunusa R., Othman N.K., Fadaiefarda F. Z. Corrosion behavior of Al6061 alloy weldment produced by friction stir welding process. *J. Mater. Res. Technol.* Vol. 4, pp. 314-322, 2015.
- [10] Friadlyander I.N., Grushko O.E., Shamrai V.F., Klochkov G.G. High-strength structural Al-Cu-Li-Mg alloy of lower density, alloyed with silver. *Metallovedenje i termicheskaya obrabotka metallov*. Vol. 6, pp. 3-7, 2007.
- [11] Holder A.E., McMurray H.N., Williams G., Scamans G. Following the Kinetics of Localised Corrosion on AA6111 Using SVET, in: *Proceedings of the 12th International Conference on Aluminium Alloys, 05-09.09.2010*, Yokohama, pp. 1475-1480.
- [12] Bardel D., Perez M., Nelias D., Deschamps A., Hutchinson C.R., Maissonette D., Chaise T., Garnier, F. Bourlier F. Coupled precipitation and yield strength modelling for non-isothermal treatments of a 6061 aluminium alloy. *Acta Mater.* Vol. 62, pp. 129-140, 2014.
- [13] Sekhar A. P., Nandy S., Ray K. K., Das D. Comparative Assessment of Strength Models for AA6063 Alloy in: *Materials Science Forum*. Vol. 880, pp. 83-89, 2016.
- [14] Sekhar A. P., Nandy S., K. K. Ray, D. Das, Artificial ageing response of an Al-Mg-Si alloy - A statistical correlation. *Perspectives in Science*. Vol. 8, pp. 739-742, 2016.
- [15] Oladele I. O., Omotoyinbo J. A. Evaluating the influence of ageing temperature on the mechanical properties of Al-Mg-Si alloy. *Journal of Minerals & Materials Characterization & Engineering*. Vol. 14, pp. 1285-1292, 2011.
- [16] Saha S., Tareq S., Galib R. Effect of Overageing Conditions on Microstructure and Mechanical Properties in Al-Si-Mg Alloy. *American Journal of Engineering Research*. Vol. 5, pp. 321-325, 2016.
- [17] Sandoval J.H., Mohamed A.M.A., Samuel F.H., Valtierra S. *International Journal Metallurgical & Materials Science and Engineering*. Vol. 5, pp. 9-1, 2013.
- [18] Wang S., Matsuda K., Kawabata T., Ikeno S. Quality performance of AL-SI-MG-CU alloys. 18 Variation of Ageing Behavior for Al-Mg-Si Alloys with Different TMs Addition in: *Proceedings of the 12th International Conference on Aluminium Alloys, 05-09.09.2010*, Yokohama, pp. 2008-2011, 2010.
- [19] GOST 10157- 79 Gaseous and liquid argon. Specifications.
- [20] Koval V.A., Labur T.M., Yavorska T.R. Properties of joints of aluminium alloy of V1341T grade in TIG welding. *Avtomatychne zvariuvania*. Vol. 2, pp. 38-43, 2020.
- [21] Rabkin D. M. Metallurgy of welding by fusion of aluminum and its alloys (Ed.): *Nauk. Dumka*, 256 p., 1986.
- [22] Nondestructive testing. Welded joints. Radiography method. GOST 7512-82.
- [23] Metals. Methods of tension test. GOST 1497-84
- [24] Welded joints. Methods of mechanical properties determination. GOST 6996-66.
- [25] Unified system of corrosion and ageing protection. Aluminium and aluminium alloys. Accelerated test methods for intercrystalline corrosion. GOST 9.021-74.
- [26] Unified system of corrosion and ageing protection. Aluminium alloys. Accelerated test method for exfoliation corrosion. GOST 9.904-82.
- [27] Unified system of corrosion and ageing protection. Aluminium and magnesium alloys. Accelerated test methods for corrosion cracking. GOST 9.919-74.

#### THE LIST OF ACRONYMS

HAZ	heat affected zone
IGC	intergranular corrosion
HT	heat treatment

#### УТИЦАЈ МИКРОСТРУКТУРЕ НА КОРОЗИЈСКО-МЕХАНИЧКУ ИЗДРЖЉИВОСТ СПОЈЕВА ЛЕГУРЕ АЛУМИНИЈУМА V1341T ЗАВАРЕНИХ РЕЛ МЕТОДОМ У ЗАШТИТНОЈ АТМОСФЕРИ АРГОНА

Љ.И. Ниркова, С.О. Осадчук, Т.М. Лабур,  
М.Р. Јаворска

Приказани су резултати утицаја микроструктуре на корозијско-механичку издржљивост легуре система Al-Mg-Si-Cu дебљине 1,2 мм и њених заварених спојева чије стање одређује врста термичке обраде. Промена микроструктуре заварених спојева услед различитих поступака термичке обраде практично не утиче на отпорност на пилинг корозију и интергрануларну корозију. Не може се са сигурношћу одредити утицај термичке обраде на корозијско-механичку издржљивост заварених спојева у условима истовременог дејства континуалног оптерећења и корозијског окружења. Отпорност на интергрануларну корозију и корозионо разарање одредиће отпорност на прелом заварених производа од легуре V1341T.